Oscillatory Rayleigh-Marangoni convection in a layer heated from above: Numerical simulations with an undeformable free surface

Thomas Boeck,[1] Matthias Jurgk,[2] and Ute Bahr[3]
[1]*Laboratoire de Modélisation en Mécanique, Université Pierre et Marie Curie (Paris VI), 8 rue du Capitaine Scott, 75015 Paris, France*
[2]*Max-Planck-Institute for the Physics of Complex Systems, Nöthnitzer Strasse 38, 01187 Dresden, Germany*
[3]*Institute for Theoretical Physics, Department of Physics, Dresden University of Technology, 01062 Dresden, Germany*
(Received 6 September 2002; published 27 February 2003)

Joint action of buoyancy and thermocapillary forces can destabilize the motionless state in a liquid layer heated from above due to the coupling of internal and surface waves. The nonlinear evolution of this oscillatory instability is studied using three-dimensional direct numerical simulations with a pseudospectral Fourier-Chebyshev code. Alternating rolls and standing, oscillating squares are observed as final convective patterns. The flow is strongly localized near the free surface. Buoyancy plays a negligible role in kinetic energy production.

DOI: 10.1103/PhysRevE.67.027303 PACS number(s): 47.54.+r, 47.20.Dr

Bénard convection has been a paradigm for pattern formation in spatially extended systems for more than a century [1–3]. Its nonlinear flow patterns continue to be the subjects in contemporary research [4]. Linear stability of the basic motionless state of the Bénard layer was explored early [3,5,6], but the interaction of certain physical mechanisms in the fluid layer still offers surprises: intuitively, neither buoyancy nor the thermocapillary effect should be able to sustain a flow in a layer with an undeformable free surface which is heated at the top. Nevertheless, an oscillatory instability exists in this case, which results from the interplay of Marangoni surface waves and internal gravity waves [7]. Both of them are damped when considered in isolation [8].

In Ref. [7], the linear theory of this peculiar instability is treated in great detail, but the investigation of the nonlinear pattern is limited to the two-dimensional case. In Ref. [1], amplitude equations are applied to the three-dimensional case. The authors derive evolution equations for the coefficients of up to 72 superimposed plane wave modes, which are then integrated numerically. It turns out that the standing two-dimensional waves found in Ref. [7] are unstable, and that (for certain parameters already considered in Ref. [7]) the system evolves towards an alternating roll pattern when the integration is started from random initial values.

Apart from actual experiments, direct numerical simulations can be used to put these predictions to the test and to overcome the restrictions of small solution amplitude inherent in the amplitude equation approach. Two-dimensional simulations have been performed previously [9]. The present paper describes results of three-dimensional direct numerical simulations for this system. We examine the horizontal and vertical flow structure as well as the kinetic energy balance of this peculiar type of convective motion.

We consider the one-layer approximation of Bénard-Marangoni convection [5]. The heat flux density q at the free surface is prescribed. Notice that q is negative in the case of heating from above. The nondimensional computational model in the domain $0 \leqslant z \leqslant 1$ with periodic boundary conditions in x and y (periodicity intervals L_x and L_y) comprises the following dimensionless equations and boundary conditions:

$$\partial_t \mathbf{v} + (\mathbf{v}\cdot\boldsymbol{\nabla})\mathbf{v} = -\boldsymbol{\nabla} p + \boldsymbol{\nabla}^2 \mathbf{v} + \mathrm{Ra}\,\theta \mathbf{e}_z, \quad \boldsymbol{\nabla}\cdot\mathbf{v} = 0, \tag{1a}$$

$$P\{\partial_t \theta + (\mathbf{v}\cdot\boldsymbol{\nabla})\theta\} = \boldsymbol{\nabla}^2\theta + v_z, \tag{1b}$$

$$\mathbf{v} = \theta = 0 \quad (\text{at } z = 0), \tag{1c}$$

$$v_z = \partial_z \theta = 0, \quad \partial_z \mathbf{v}_h = -\mathrm{Ma}\boldsymbol{\nabla}_h \theta \quad (\text{at } z = 1). \tag{1d}$$

Equations (1) for the velocity $\mathbf{v}$, the pressure p and temperature perturbation θ are based on the layer thickness d as unit of length, d^2/ν as unit of time, and qd/λ as unit of temperature, where λ denotes the heat conductivity of the fluid. The Prandtl number $P = \nu/\kappa$ represents the ratio of kinematic viscosity and thermal diffusivity. The full nondimensional temperature is defined by $T = P\theta + 1 - z$, and the Marangoni and Rayleigh numbers by $\mathrm{Ma} = \gamma q d^2/\lambda\rho\nu\kappa$ and $\mathrm{Ra} = \alpha g q d^4/\lambda\nu\kappa$. Here ρ denotes the density, α the thermal expansion coefficient, and $\gamma = -d\sigma/dT$ is the (negative) derivative of the surface tension with respect to temperature. The subscript h indicates the horizontal part of a vector.

We solve the system (1) numerically using a pseudospectral Fourier-Chebyshev discretization based on the poloidal-toroidal decomposition of the velocity field [10]. This discretization provides a dense vertical spacing of the collocation points at the top and bottom boundaries, and should therefore be capable of resolving strong gradients even with a moderate number of modes. The method is based on that presented in Ref. [11] for $\mathrm{Ra} = 0$. Time stepping is done using the explicit, second-order Adams-Bashforth method for the nonlinear terms. For the linear terms (including the buoyancy term), an implicit method ensures numerical stability. The second-order accuracy is desirable to avoid severe limitations in the size Δt of the time step, but the Crank-Nicolson method turned out to be weakly unstable. It was replaced by the less accurate but more stable ϑ method [12]. The code was validated with respect to the nonlinear terms by comparison with nonlinear simulations of Bénard-Marangoni convection at low Prandtl number (with $\mathrm{Ra} = 0$, $\mathrm{Ma} = 80$) [11] and with respect to the linear terms by reproducing the growth rate λ of the stationary instability for heating from below [6] with a relative error of 6×10^{-7} using 33 Chebyshev polynomials ($\mathrm{Ra} = 400$, $\mathrm{Ma} = 50$, wave number $k = 1.5$, $P = 6$, time step $\Delta t = 10^{-3}$, $\lambda = 0.071\,187\,19$).

In experiments, the heat flux density q can be easily var-

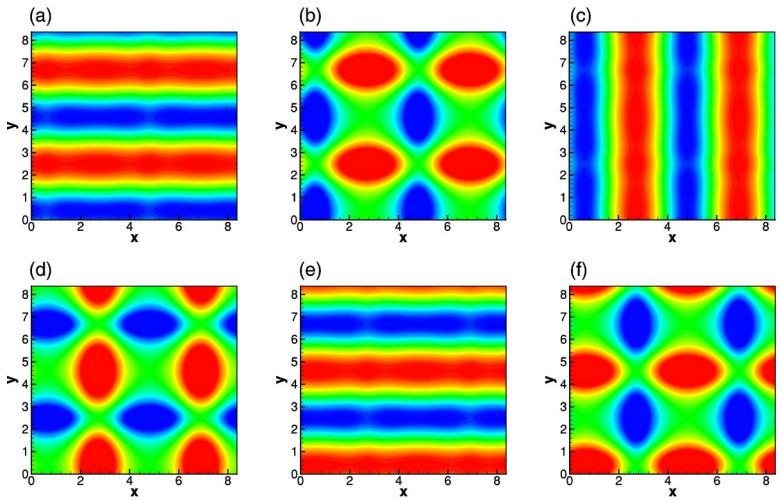

FIG. 1. Surface temperature of alternating rolls ($P=6$,Ma$=-6.0\times10^5$,$B=3$). Interval between snapshots is $\Delta t=0.0028$.

ied in contrast to d or the fluid itself, i.e., $B=\mathrm{Ra}/\mathrm{Ma}$ (the dynamic Bond number) and P are fixed for a given setup. We take the same approach in our simulations and consider parameters already studied in Ref. [7], namely, $P=6$ and $P=0.1$ and values of B in the interval $3\leqslant B\leqslant 10$. For $P=6$ and $B=3$, the critical wave number is $k_c=1.506$ at $\mathrm{Ma}_c=-4.116\times10^5$. It is desirable to select large multiples of the corresponding critical wavelength for the horizontal dimensions of the computational domain in order not to constrain the pattern. The computational workload as a limiting factor grows with the domain size due to the correspondingly larger grid and possibly longer initial transients. We have taken $L_x=L_y=4\pi/1.5$ as a compromise.

We shall first discuss our results for $P=6$, where we obtained alternating roll patterns in the cases $B=3$, $B=4$, and $B=5$ when starting from random initial conditions. This kind of pattern results from the superposition of two orthogonal plane standing waves and is a generic pattern for the Hopf bifurcation on a square lattice [13].

Figure 1 shows six snapshots of the surface temperature for alternating rolls and Fig. 2(a) shows the corresponding temporal evolution of the (Fourier) amplitudes of the two standing waves generating this pattern, which have a relative phase shift of $\pi/2$. The first five plots of Fig. 1 represent half of the total period $2\pi/\omega$, where ω is the frequency of the basic oscillation. The second half period (not shown) is analogous to the first except for spatial shifts of half a wavelength in both x and y directions. We note that the temporal phase shift of $\pi/2$ between the two amplitudes does not mean that pure rolls exist at any time during the evolution. Figure 2(b) shows the evolution of the kinetic energy components E_x and E_y defined by

$$E=E_x+E_y+E_z=\frac{1}{2}\int_\Omega (v_x^2+v_y^2+v_z^2)d\Omega, \qquad (2)$$

where Ω denotes the periodicity domain. The quantities E_x and E_y are always positive, i.e., the flow is never independent of either x or y at any time. The persistence of three-dimensionality is due to the oscillatory nature of the instability (which requires complex eigenmodes of the linear stability problem). The ratio between the maximum and minimum values of E_x and E_y is indicative of the variation of the complex, z-dependent phase of the marginally stable mode (near the instability threshold Ma_c) [14].

The orientation of the pattern is not necessarily parallel to the coordinate axes. Starting from random initial conditions we have also found a pattern with oblique orientation corresponding to the wave number $k=1.677$, whereas the parallel pattern has the basic wave number $k=1.5$.

To characterize the alternating rolls quantitatively, we have measured the oscillation frequency ω and the temporal average of kinetic energy E as function of Ma for ($P=6$, $B=3$) for $k=1.5$. Figure 3(b) shows the relation $\omega(\mathrm{Ma})$, which is quantitatively well captured by the linear theory of the basic state. The relation $E(\mathrm{Ma})$ plotted in Fig. 3(a) is well fitted by a straight line. Extrapolation to $E=0$ provides $\mathrm{Ma}=-4.14\times10^5$, which is only slightly off the critical value Ma_c. Both observations suggest that a description us-

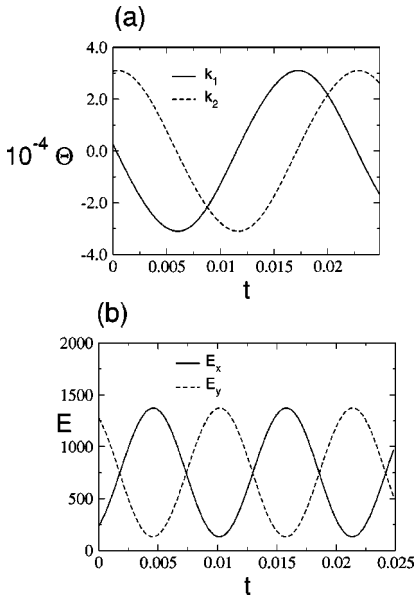

FIG. 2. Alternating rolls with $P=6$, Ma$=-6.0\times10^5$, $B=3$: (a) Amplitudes of the two orthogonal waves with wave vectors $\mathbf{k}_1$ and $\mathbf{k}_2$. (b) Energy components E_x and E_y.

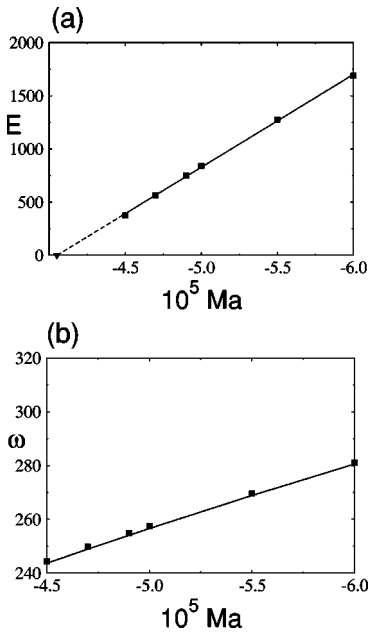

FIG. 3. Temporal mean of kinetic energy E (a) and angular frequency ω (b) for orthogonal alternating rolls with basic wave number $k=1.5$ and $P=6$, $B=3$. The full line for ω corresponds to the prediction from linear theory (differs by factor $1/2\pi$ from data in Refs. [7,1]).

ing a perturbative or amplitude equation approach can provide a quantitative description of the flow in the range explored by our simulations. We remark that these simulations were performed with 64 Fourier modes in the horizontal directions and 33 Chebyshev modes in the vertical direction. Visual inspection of vorticity plots showed no indication of small scale features indicative of spatial under-resolution. The high oscillation frequencies of the solutions require fairly small values for the time step. Initially, $\Delta t=10^{-4}$ was used, which was decreased to $\Delta t=10^{-5}$ upon approach to the final state. The corresponding change in E due to this smaller Δt was about 10%. Another order of magnitude decrease of Δt changed E by less than 1%.

The spatial structure of the flow is illustrated by the plots of Fig. 4. We see from Fig. 4(a) that the isotherms in the plane $y=0$ are only slightly disturbed by the convective motion. Figure 4(b) shows the horizontal mean square averages of the velocity components. Large vertical gradients of the horizontal velocity exist near the free surface, which are expected from linear theory [7]. The presence of such strong gradients underlines the utility of our Fourier-Chebyshev numerical method. Steep vertical gradients of the temperature perturbation θ near the free surface are also predicted by linear theory, but they do not show up in Fig. 4(a) due to the small overall amplitude of θ. The change in the average surface temperature is less than 10^{-2}, i.e., the convective heat transport by the flow is insignificant.

The case $P=0.1$ presented significant numerical problems due to long transients and higher vertical resolution requirements (65 Chebyshev modes instead of 33). This is because the flow is even more strongly localized near the free surface than for $P=6$. We have only obtained one fully converged simulation with $P=0.1$,$B=10$ shown in Fig. 5. The pattern is different from $P=6$, namely, standing, oscillating squares.

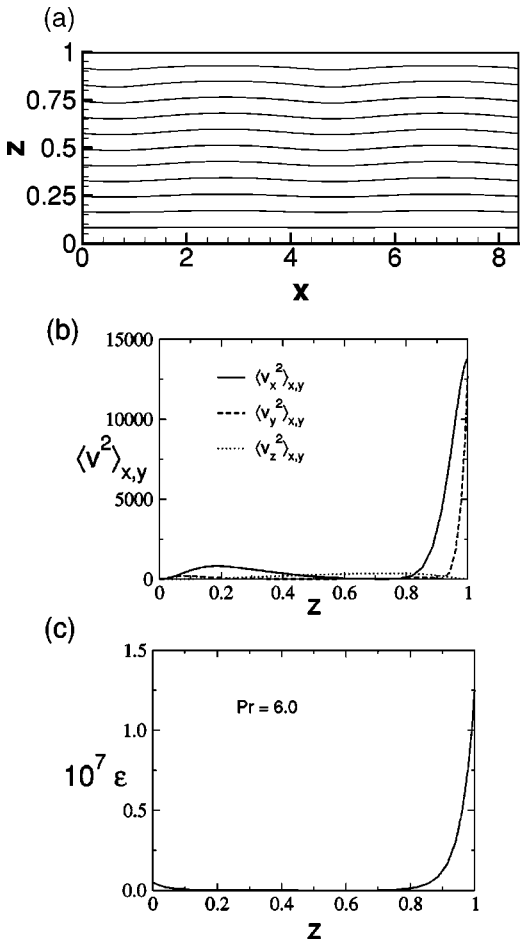

FIG. 4. Typical snapshots for parallel alternating rolls with $P=6$, $\mathrm{Ma}=-6.0\times10^5$, $B=3$. (a) Temperature in $y=0$ plane; vertical profiles of mean square velocity components (b) and energy dissipation rate ε (c) (both horizontal means).

The two orthogonal standing waves making up this pattern are parallel to the coordinate axes. The wave vectors have the size $k=1.5$, and the wave amplitudes are oscillating in phase [Fig. 5(b)]. The critical parameters from Ref. [7] are $\mathrm{Ma}_c=-5.54\times10^4$, $k_c=1.501$ for $P=0.1$, and $B=10$. We have not attempted to trace the solution to other values of Ma because of long transients. Other simulations for $P=0.1$ with larger aspect ratio also showed a preference of the standing, oscillating squares although these patterns had defects which persisted during the limited simulation times.

To conclude our discussion on the numerical results, we now consider the energy balance. Kinetic energy can be generated from buoyancy and Marangoni forces. After inital transients, the kinetic production equals dissipation through viscosity over an oscillation period. The energy balance is obtained by multiplying the Navier-Stokes Equation (1a) by $\boldsymbol{v}$ and integration over the fluid volume Ω. We find

$$\mathrm{Ma}\left\{\int_{z=1}\mathbf{v}_h\boldsymbol{\nabla}_h\theta dS+B\int_\Omega v_z\theta d\Omega\right\}=-\int_\Omega\frac{\varepsilon}{P}d\Omega, \quad (3)$$

where ε denotes the local energy dissipation rate. The terms on the left hand side of Eq. (3) are the production terms of thermocapillary effect and buoyancy. Buoyancy turns out to be negligible in this relation, the buoyancy terms is by four

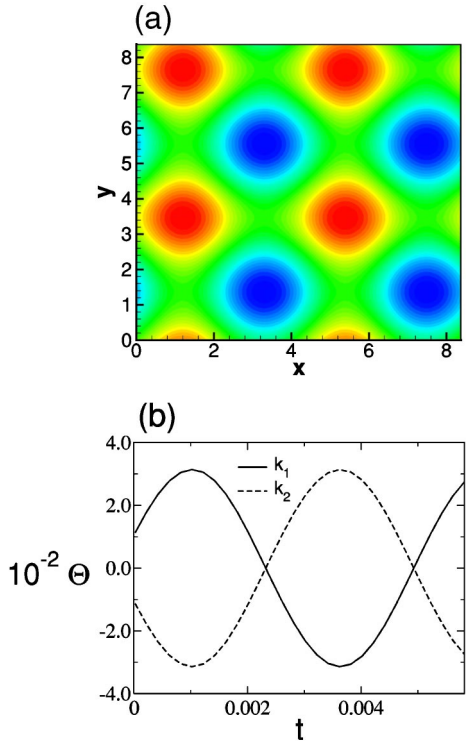

FIG. 5. Standing squares for $P=0.1$, $\mathrm{Ma}=-5.94\times10^4$, $B=10$: (a) Surface temperature snapshot; (b) amplitudes of the two orthogonal waves with wave vectors $\mathbf{k}_1$ and $\mathbf{k}_2$.

orders of magnitude smaller than the Marangoni term for $P=6$. In the converged state for $P=0.1$ it is smaller by a factor of about 10^{-10}. The dissipation is strong in regions with strong velocity gradients, i.e., near the free surface. Figure 4(c) shows a representative vertical profile of ε (averaged horizontally) for $P=6$.

The negligible role of the buoyancy term in the energy budget can be understood from the asymptotic analysis of the linear stability problem in Ref. [7]. In this asymptotic analysis in the small parameter $\epsilon^4=-P/\mathrm{Ra}$, the linear problem is solved separately in the bulk and in a surface layer, which are then matched to provide the dispersion relation. The horizontal velocity in the surface boundary layer has a leading term of order ϵ^{-1}, whereas the temperature perturbation and the vertical velocity have leading order ϵ^0. The terms in the energy budget containing the horizontal velocity components, namely, the Marangoni energy production and the viscous dissipation term, are therefore much bigger than the buoyancy term, to which the horizontal velocity does not contribute.

In summary, we have performed three-dimensional simulations of convective flow in a plane layer heated from above driven by the oscillatory instability mechanisms discovered by Rednikov *et al.* [7]. The simulations were performed with a pseudospectral Fourier-Chebyshev code. A sufficiently accurate temporal discretization using the ϑ method with $\vartheta\approx0.5$ for the linear terms was required to reproduce the predicted instability without prohibitively small time steps in the simulations. The observed flow patterns turned out to be alternating rolls for $P=6$ and standing, oscillating squares for $P=0.1$. The vertical flow structure and the energy balance are in accord with linear stability theory and its asymptotic solution.

An interesting open problem to be addressed in the framework of amplitude equations concerns the domains of existence of alternating rolls and standing squares in the parameter space and the stability of those patterns. Equally or more important is the need for experimental work. Alternating roll patterns have to our knowledge only been obtained in simulations or analytical work on compressible magnetoconvection [15,16], two-layer Marangoni convection [14], and the Maxwell-Bloch laser equations [17].

We are grateful to M. Bestehorn and A. Nepomnyashchy for interesting discussions and to the Zentrum für Hochleistungsrechnen at Dresden University of Technology for the extensive use of its parallel computers.

[1] P. Colinet *et al.*, *Nonlinear Dynamics of Surface-Tension-Driven Instabilities* (Wiley-VCH, Berlin, 2001).
[2] E.L. Koschmieder, *Bénard Cells and Taylor Vortices* (Cambridge University Press, Cambridge, 1993).
[3] S.H. Davis, Annu. Rev. Fluid Mech. **19**, 403 (1987).
[4] M.F. Schatz and G.P. Neitzel, Annu. Rev. Fluid Mech. **33**, 93 (2001).
[5] J.R.A. Pearson, J. Fluid Mech. **4**, 489 (1958).
[6] D.A. Nield, J. Fluid Mech. **19**, 341 (1964).
[7] A.Y. Rednikov *et al.*, J. Fluid Mech. **405**, 57 (2000).
[8] To visualize the (longitudinal) surface wave, imagine a spatially periodic disturbance of the surface temperature. Marangoni forces will carry hot fluid to the cold spots. Fluid inertia causes overshoot, i.e., the former warm spots will now be cold and vice versa. Displacing fluid elements vertically can increase the potential energy, e.g., by a deformation of the interface between a lighter upper and a lower, more dense fluid. The restoring body force drives the interface back, and inertia causes overshoot. These so-called internal gravity waves are transverse and occur also for a continuous density gradient. Thermal diffusion and viscous dissipation hinder wave motion.
[9] D. Merkt, diploma thesis, University of Stuttgart, 1998.
[10] C. Canuto *et al.*, *Spectral Methods in Fluid Dynamics* (Springer, Berlin, 1988).
[11] T. Boeck and A. Thess, J. Fluid Mech. **399**, 251 (1999).
[12] K.W. Morton and D.F. Mayers, *Numerical Solution of Partial Differential Equations* (Cambridge University Press, Cambridge, 1994).
[13] M. Silber and E. Knobloch, Nonlinearity **4**, 1063 (1991).
[14] T. Boeck *et al.*, Phys. Fluids **14**, 3899 (2002).
[15] Th. Clune and E. Knobloch, Physica D **74**, 151 (1994).
[16] P.C. Matthews *et al.*, J. Fluid Mech. **305**, 281 (1995).
[17] Q. Feng *et al.*, Phys. Rev. A **50**, R3601 (1994).